Title: **Direct Interaction of FtsZ and MreB is Required for Septum Synthesis and Cell Division in *Escherichia coli***

Authors: Andrew K. Fenton and Kenn Gerdes

Address: Centre for Bacterial Cell Biology, Baddiley-Clark Building, Medical School, Newcastle University, Richardson Road, Newcastle-upon-Tyne, NE2 4AX, United Kingdom

Supplemental Information

Supplementary Materials and Methods

Strains and Growth media

For all strains and plasmids used in this study see supplementary Table SI. Typically cultures were raised in 5 ml LB (10 g/l tryptone [Oxoid], 5 g/l yeast extract [Oxoid] and 10 g/l NaCl [AnalaR Normapur]) and incubated shaking for at least 16 h at 30^{o}C using antibiotics: ampicillin (50 μg/ml), kanamycin (25 μg/ml), chloramphenicol (25 μg/ml) or tetracycline (20 μg/ml) [Sigma-Aldrich] where appropriate. Nutrient Agar (NA) medium was used for all agar plates [Oxoid]. M9 media was used for all microscopy and growth experiments and was made fresh from autoclaved stock components (Na_2HPO_4 0.6 g/l, KH_2PO_4 0.3 g/l, NaCl 0.05

g/l, NH_4Cl 0.1g/l, 0.2% w/v casamino acids [Bacto Difco], 0.001% w/v thiamine [Sigma-Aldrich], 1 mM $CaCl_2$, 1 mM $MgS0_4$, pH = 7.4, chemicals from AnalaR Normapur unless otherwise stated). Glycerol (0.5% v/v, [GPR Rectapur]) was typically used as a carbon source however glucose (0.4% w/v, [Formedium]) was occasionally used where indicated.

Epi-fluorescence microscopy

All epi-flourescence microscopy was carried out using an Olympus 1X71 inverted microscope pre-heated and maintained at 30^{o}C using a Precision Control environmental chamber. Images were taken through a 100X Zeiss Plan-NEOFLUAR oil objective (NA 1.3) using a Photometrics CoolSNAP HQ CCD camera combined with the softWoRx software (version 5.5 or 3.5.1). Epi-fluorescence images were acquired using an Olympus 100W Mercury burner (U-LH100HG) light source with 'FITC' (Ex 490/20, Em 528/38 nm), 'RD-TR-Cy3' (Ex 555/28, Em 617/73 nm) and 'DAPI' (Ex 360/40, Em 457/50) filter-sets [Chroma]. For time-lapse microscopy focal position was maintained using the Applied Precision UltimateFocus^{TM} system in conjunction with a Applied Precision Nanomotion X,Y,Z stage, sampling every 10 s. Final Image preparation was performed in ImageJ (1.44o).

Development of the mYpet-MreB functional fusion

To fluorescently tag MreB we used the YPet fluorophore due to its high brightness (Nguyen & Daugherty, 2005). To form a functional N-terminal tagged YPet-MreB recombinant protein, the first methionine residue was removed from full length MreB and a series of linker regions between the two domains were tested, based on those described in (Arai *et al*, 2001). Constructs were assayed for their ability to complement a MC1000 *ΔmreB*

strain, restoring its spherical morphology to wild-type rods. One construct was shown to maintain both growth rate and restore viability in *mreB* depletion assays described in (Kruse *et al*, 2005).

The final chosen construct used in this study had a linker region which codes for the amino acids: GPGPI. This linker region sits between the *ypet* and *mreB* ORF, the final fusion protein coding K-GPGPI-L [AAG-GTCCAGGGCCCATCT-TGA], where 'K' is the final lysine residue of Ypet and 'L' is the second leucine residue of full-length MreB.

Finally the YPet fluorescent protein was further engineered introducing the A206K mutation to prevent any potential localisation artefacts resulting from fluorophore dimerisation and re-named: mYpet (Zacharias *et al*, 2002).

mYpet-MreB septal localisation microscopy

MG1655 pAKF106 (P_{BAD}::*mYpet-mreB*) stationary-phase cultures were diluted 1/100 into 25 ml M9 glucose with 0.05% arabinose in a 125 ml conical flask. Under these conditions induction of the P_{BAD} promoter was minimal and did not affect growth rate or cell morphology (see Figure S1A). Resulting mixtures were incubated for 3 h at 30^{o}C, typically giving OD_{600} values of between 0.29 and 0.33. Culture samples were spotted onto pre-set 1% M9 glucose pads which had been pre-equilibrated to 30^{o}C and imaged immediately for both single image analysis and time lapse microscopy. The same conditions were used for microscopy involving the FB76 (*mreB-RFP*^{SW}) strain (see Figure S1F,G).

MreB and FtsZ septal localisation Immuno-Fluorescence Microscopy (IFM)

MG1655 stationary-phase cultures were diluted 1/100 into 25 ml M9 glucose supplemented with 0.05% arabinose in a 125 ml conical flask. Resulting mixtures were

incubated for 3 h at 30^{o}C. Two 500 µl aliquots of cell culture were fixed by adding 500 µl of 'fixation solution' (2% formaldehyde, 0.2% glutaraldehyde in PBS [phosphate buffered saline, pH 7.3, Oxoid]) and incubated for 20 min at room temperature followed by a further 40 min incubation on ice. Cells were washed three times in 500 µl PBS and permeabilized by re-suspending both cell pellets in 150 µl of freshly prepared lysozyme solution (100 µg/ml lysozyme from chicken egg white [Sigma-Aldrich], 5 mM EDTA in PBS); mixtures were incubated for 45 min at room temperature. Cells were washed twice in 150 µl PBS, pelleting each time at 6,000 g for 6 min. Non-specific binding sites were blocked by re-suspending cell pellets in 150 µl blocking solution (5% milk powder in PBS) and incubating at 37^{o}C for 30 min. Primary rabbit anti-MreB antibody was diluted 1,000 fold in blocking solution and 150 µl added to the mixture, cells were incubated at 37^{o}C for 1 h (Kruse *et al*, 2003). An antibody specificity Western blot for the anti-MreB is shown in Figure S1E. Cells were washed three times in 500 µl PBST (PBS +0.05% v/v Tween). Secondary FITC-conjugated-anti-rabbit-goat IgG antibody [Sigma-Aldrich] was diluted 600 fold in blocking solution and 150 µl used to re-suspend cell pellets. This mixture was incubated in the dark at 37^{o}C for 30 min. Cells were washed in PBST as before and finally re-suspended in 100 µl PBS and imaged immediately.

For anti-FtsZ IFM the same detection procedure was followed, using rabbit anti-FtsZ primary antibodies diluted 1,000 fold (Galli & Gerdes, 2012; Kruse *et al*, 2003) and secondary Alexa 568 Goat anti–rabbit IgG antibodies [Molecular probes] diluted 300 fold for detection.

Bacterial Two-Hybrid (BTH) analysis

In order to find protein factors responsible for MreB-Z ring recruitment we used a BTH screen against a pre-existing library of cell division factors (Karimova *et al*, 2005).

Plasmids used for BTH analysis were transformed into the BTH101 strain and transformants selected on NA plates containing selective antibiotics and 40 µg/ml 5-bromo-4-chloro-3-indolyl-β-D-galactopyranoside (X-gal) incubating at 30^{o}C for 24-48 h. For each plasmid combination two or three transformants were selected, grown to stationary phase in LB and 5 µl spotted onto NA +antibiotics +X-gal to test signal robustness. Representative transformants were used for the large BTH screen plates. Plates were scanned on an Epson perfection V700 photo flatbed scanner. Measurements of β-galactosidase activity in liquid media were performed on 1 ml aliquots of growth-phase cultures as described in (Miller, 1972).

MreB-FtsZ *in vivo* formaldehyde cross-linking

His_8-tagged MreB and $MreB^{D285A}$ were expressed from plasmids pTK500 and pAKF126 respectively without induction in MC1000. 4 ml stationary phase cultures were used to inoculate 400 ml of M9 media, incubated at 30^{o}C shaking for 4 h reaching an OD_{600} of between 0.5 and 0.6. Proteins were cross-linked by the addition of formaldehyde (1% final concentration) and quenched after 10 min using 150 mM glycine. Tagged and cross-linked MreB was purified from cell pellets under denaturing conditions in 3 ml UT-buffer [0.1 M HEPES, 0.5 M NaCl, 50 mM Imidazole, 8 M Urea, 1% Triton X-100, 1 mM Dithiothreitol, 1 mM Phenylmethanesulfonylfluoride] by adding 50 µl of MagneHis^{TM} Ni-Particle suspension (Promega) as described in (Ishikawa *et al*, 2006). The particles were washed in UT buffer and protein complexes were eluted in 200 µl of elution buffer [0.1 M Tris-HCl, 0.5 M Imidazole, 1% SDS, 10 mM Dithiothreitol] and concentrated by centrifugation using a Amicon Ultra – 0.5 ml Centrifugal Filter [Millipore]. Complexes were washed three times in 400 µl of M-wash buffer [0.1 M Tris-HCl, 1% SDS, 10 mM Dithiothreitol] using the

filter. Protein cross-links were reversed by incubating preparations at 95^{o}C for 1 h. Equal volumes of protein preparations were loaded onto 4-12.5% SDS-PAGE gels and individual proteins detected by Western blot using anti-FtsZ and anti-MreB antibodies [both used at a 1/10,000 dilution] (Galli & Gerdes, 2012; Kruse *et al*, 2003).

His-MreB and FtsZ protein purification

Native FtsZ was purified exactly as described in (Galli & Gerdes, 2012). His_8-MreB was overexpressed from pTK500 in MC1000 *E. coli* cells. Stationary phase cultures were diluted 1/100 in 400 ml LB, incubated for 3 h at 37^{o}C and induced with 2 mM isopropyl-β-D-thiogalactopyranoside (IPTG). After 3 h of continued incubation, cells were harvested by centrifugation (6,400 g, 10 min) and re-suspended in bufferA (50 mM Sodium phosphate, 0.5 M NaCl, 20 mM imidazole, pH 7.5) using a ratio of 5 ml/g of pellet. Cells were lysed by incubation with 1 mg/ml lysozyme for 1h on ice and sonication using a Sonics Vibra-cell^{TM} sonicator (0.6 W, 1 s pulses for 5 min). Cell debris was removed by centrifugation (6,400 g, 15 min and two 40,000 g for 20 min spins) and supernatant loaded onto a pre-equilibrated 1 ml HisTrap HP collum [GE Healthcare]. After washing, His_8-MreB was eluted from the collum using stepwise increments of bufferB (bufferA + 0.5 M imadazole). Purified protein was dialysed into storage buffer (50 mM Sodium phosphate, 0.5 M NaCl, 20% v/v glycerol, pH 7.5).

MreB depletion microscopy

The MC1000Δ*mre*,pTK549,pKG339 MreB depletion system was used as described in (Kruse *et al*, 2005). A diagram summarising how this system works can be found in Figure S4A. Briefly, stationary phase cultures were diluted 1/100 in fresh LB +tetracycline, 2mM

IPTG (for depletion) and 0.2% arabinose for MreB or MreB^{D285A} expression from pAKF128 (P_{BAD}::*mreBCD*) or pAKF129 (P_{BAD}::*mreB^{D285A}CD*) respectively. Mixtures were incubated at 30^{o}C for 3 h and imaged immediately. Cells overexpressing the *mreBCD* operon or cells which had failed to complement were excluded from the analysis (approximately 10-15% of cells). In addition, cells that failed to complement the *Δmre* phenotype due to MreBCD dosage effects through phenotype complementation were also excluded (approximately 6-8% of cells).

mYpet-MreB – MreB-RFP^{SW} co-localisation microscopy

Stationary phase cultures of the MreB-RFP^{SW} strain: FB76 containing pAKF131 or pAKF132 (P_{BAD}::*mYpet-mreB/mreB^{D285A}*) were diluted 1/100 into 25 ml M9 media supplemented with antibiotics. Cells were induced with 0.15% arabinose after a 2 h shaking incubation at 30^{o}C and incubated for a further 3 h. A similar protocol was used when detecting mYpet-MreB fusion proteins expressed from pAKF131 or pAKF132 in MC1000. Growth rate and cell morphology were perturbed under our minimal media growth conditions used for microscopy, making this strain unsuitable for further work in this study (Figure S1A).

Bacterial two-hybrid FtsZ point mutagenesis screen

An error-prone PCR using a modified Pfu(exo^{-})D473G polymerase and primers: AKF_FtsZ_pKNT25_F (GCCAAGCTTGCATGCCTGCAGGTCG) and AKF_FtsZ_pKNT25_R (AGCTCGGTACCCGGGGATCCGG) were used to amplify the *ftsZ* ORF from pKNT25-ftsZ exactly as described in (Biles & Connolly, 2004). PCR products were digested with both HindIII and BamHI, ligated into pKNT25-ftsZ (cut with the same enzymes) and transformed

into BTH101 pUT18-mreB(D285A). Candidates which consistently gave blue cultures on NA plates containing X-gal (40 mg/ml) were selected and both plasmids in these strains separated by transformation into DH5α. Re-isolated pUT18C-mreB(D285A) plasmids were diagnostically digested with MmeI to screen out possible reversion mutants. Re-isolated pKNT25-*ftsZ*-mutant plasmids were co-transformed into BTH101 strains with either: pUT18-ftsZ, pUT18C-mreB or pUT18C-mreB(D285A) to confirm the initial D285A 're-binding' phenotype and check protein variants could still bind FtsZ (see Figure S5A). Finally all mutants were sequenced using: DNA Sequencing and Services, Dundee.

HADA fluorescent D-amino acid cell wall labelling

Live *E. coli* cell wall labelling was carried out essentially as described in (Kuru *et al*, 2012). *E. coli* MC100 cells were grown in M9 media for microscopy as described above. After 5 h of incubation at 30^{o}C a 450 µl aliquot of culture was taken and the cell wall labelled by adding 5 µl of 100 mM HADA dissolved in DMSO. This gave a final concentration of 1.1 mM HADA in 1.1% DMSO. Cells were incubated for 30 seconds before pelleting at 5 g for 1 min. Cell pellets were immediately fixed using 500 µl of ice cold 70% ethanol and incubated on ice for 20 min. Cells were washed three times by repeated centrifugation at 17 g and re-suspension in 500 µl PBS (pH 7.6), samples were stored at 4^{o}C. For microscopy, cells were mounted on 1% agarose PBS pads and imaged using the 'DAPI' filter set.

Supplementary Figure Legends

Figure S1. Growth curves, cell morphology controls, Western blot controls and supporting IFM and fluorescence microscopy for MreB-septal localisation detection. (A) (i) Growth curves of MG1655 pAKF106 (P_{BAD}::*mYpet-mreB*) expressing mYpet-MreB at increasing concentrations of arabinose inducer. A FB76 (MG1655 Δ*lacIZYA*, *mreB-RFP*^{SW}) growth curve is also shown; this strain expresses the MreB-RFP^{SW} fusion protein from the native P_{mre} promoter on the genome. All strains were incubated shaking at 30^{o}C in M9 glucose media. (ii) Representative bright field micrographs of MG1655 pAKF106 cells at 0.05% and 0.2% arabinose showing loss of cell morphology when mYpet-MreB is overexpressed. Note a final concentration of 0.05% arabinose does not affect MG1655 growth rate or morphology. **(B)** Representative Western blot of MG1655 cells expressing mYpet-MreB from pAKF106 (P_{BAD}::*mYpet-mreBCD*). Cells were grown in the same conditions used for mYpet-MreB fluorescence microscopy (M9 glucose, 30^{o}C, 3 h incubation, +/- 0.05% arabinose inducer). Resulting cultures were matched by OD_{600}, concentrated 10 fold and used for Western blotting using rabbit anti-MreB antibodies. Location of 37 and 50 kD marker bands are highlighted. For quantifications three independent samples of mYpet-MreB band intensities were measured at least three times and compared to the wt MreB band and averaged. MreB band intensities between conditions were not statistically different (t-test, $p>0.4$). **(C)** Selected bright field and anti-MreB IFM images of MG1655. Representative examples of both non-dividing and dividing cells at differing stages of cell division are shown. **(D)** Combined anti-MreB IFM and fluorescence-micrographs of MG1655 expressing FtsZ-mCherry from pQW59. Merged images reveal IFM-MreB signals co-localise with FtsZ-mCherry with a frequency of 68% (117 Z rings scored, n=3) **(E)** MreB Western blot of a

MG1655 lysate, shown as a control for the confidence in Immunofluorescence localisation patterns shown in parts C and D. Cells were grown and concentrated as described in (B). Note that >85% of the signal in the entire lane was present in the MreB band. The top and bottom of the membrane has been indicated **(F)** Brightfield and fluorescent micrographs of FB76 (P_{mre}::*mreB-RFP*^{SW}) grown in M9 glucose media for 3 h at 30^{o}C. (i) Examples of a dividing and non-dividing cell. Note no MreB 'band' in the non-dividing cell vs the MreB signal at mid-cell in the dividing cell. Cells shown are not typical examples as cell morphology is often perturbed in this strain under these growth conditions and are shown here solely to indicate that MreB-RFP^{SW} can be recruited to mid-cell. (ii) Typical population of FB76 grown in M9 glucose. Note cell morphology in some cells is somewhat wider than expected, indicating a possible loss of cytoskeletal function. MreB bands are highlighted with red arrows. **(G)** FB76 strain containing the pDWS230 (P_{lac}::*ftsZ-gfp*) plasmid. Cells were grown in the same conditions used for mYpet-MreB fluorescence microscopy. Positions of overlapping MreB bands and FtsZ signal have been indicated using arrows. Cell shown is not typical, as often cell morphology in this strain under these conditions is adversely affected and is shown here to indicate that MreB-RFP^{SW} and FtsZ-GFP signals can overlap in a way similar to that of mYpet-MreB or anti-MreB immunofluorence and FtsZ-mCherry (see part D and Figure 1B). Scale bars = 5 μm (A,F) or 2 μm (C,D,E).

Figure S2. mYpet-MreB forms bands in *ftsA*^{ts} strains but not in *ftsZ*^{ts} cells at non-permissive temperatures. Representative bright field and fluorescent micrographs of temperature sensitive *E. coli* cells expressing GFP tagged MreB and FtsZ fusion proteins. Cells were diluted 1/100 and grown in M9 glucose medium with 0.05% arabinose inducer. Cultures were incubated for 1 h at 30^{o}C before being shifted to permissive (30^{o}C) and non-

permissive (42^{o}C) temperatures for 2 h. **(A)** *ftsZ*^{ts} strain PS106 (*ftsZ84 leu::*Tn*10* (Ts)), pAKF106 (P_{BAD}::*mYpet-mreBCD*) in which non-active FtsZ protein was detected by IFM. Fixed and stained cells were spotted onto a 1% PBS aragose pad for imaging. **(B)** *ftsA*^{ts} strain PS236 (W3110: *ftsA12 leu::*Tn*10* (Ts)), pAKF106 (P_{BAD}::*mYpet-mreBCD*), pQW59 (P_{lac}::*ftsZ-mCherry*). Cells were spotted onto a 1% M9 aragose pad and images live. Note: co-localising mYpet-MreB – FtsZ signals can be detected in *ftsA*^{ts} strains at any temperature, but are lost from *ftsZ*^{ts} strains at non-permissive temperatures. Scale bars = 5 µm.

Figure S3. MreB-FtsZ bacterial two hybid self-interaction controls, antibody affinity assays and MreB overexpression viability tests. (A) Bacterial-two-hybrid (BTH) results showing FtsZ and MreB self-interactions are maintained when labelled in different contexts: (i) FtsZ is tagged C-terminally vs N-terminally (shown in brackets), (ii) with a 9 amino acid N-terminal truncation of MreB (ΔN) and (iii) the constructs contain the MreB^{D285A} mutation. Cells were spotted onto NA plates containing: ampicillin (50 µg/ml), kanamycin (25 µg/ml) and X-gal (40 µg/ml) and incubated for 36 h at 30^{o}C prior to imaging (n=3). BTH –ve control strains contained empty pKNT25 and pUT18 vectors and +ve control strains contained the pKT25-zip and pUT18C-zip fusions. In all cases the BTH101 strain was used for these assays, full details of all plasmids used are available in Table SI. **(B)** Representative Western blots showing anti-FtsZ or anti-MreB antibodies do not cross-react (n=3). Western blot performed on purified FtsZ and His-MreB preparations and loaded in the amounts indicated above each lane. **(C)** Structural model of MreB from *T. maritima* highlighting the position of the *E. coli* 285 Aspartate (Asp) residue (highlighted in black). The D285 residue of *E. coli* MreB corresponds to the Asp 275 residue of MreB in *T. maritima*. MreB domains have been

labelled and coloured as in: (Van den Ent *et al*, 2001). **(D)** CFU counts of *E. coli* MC1000 cells containing: pBAD24 (empty vector), pAKF128 (P_{BAD}::*mreBCD*) or pAKF129 (P_{BAD}::*mreB*^{D285A}*CD*) over expression constructs. 5 µl of 1/10 serial dilutions of cultures were spotted onto M9 agar plates with different concentrations of arabinose inducer. Plates were incubated for 16 h at 30^{o}C prior to imaging. Plates shown are from the same experiment and are representative of two independent repeats which gave identical results. Note: the arabinose concentration of 0.000,05% used for all MreB 'overexpression' microscopy does not affect CFU counts.

Figure S4. MreB depletion system schematic and Western blot. Representative MreB and MreB^{D285A} overexpression images and cell width controls.

(A) Diagrammatic representation of the three-plasmid MreBCD depletion system. An MC1000 Δ*mreBCD* strain was complemented by pTK549 (P_{mre}::*mreBCD*), a low-copy-number R1 plasmid (≈1 copy per genome). Addition of IPTG induces expression of the antisense RNA *copA* encoded by pKG339, thereby inhibiting replication of the complementing R1 plasmid. The pTK549 plasmid and MreBCD proteins are rapidly lost through protein turnover and dilution by cell growth and division. Expression of an *mreBCD* operon under P_{BAD} control carried by a third plasmid (pAKF128 in this example) allowed the study of lethal *mreB* mutant phenotypes. Cm^{r}, Tet^{r}, Kn^{r} and Amp^{r} antibiotic markers confer: chloramphenicol, tetracycline, kanamycin and ampicillin resistance respectively. **(B)** Western blot of the MreBCD depletion system detailed in (A) using rabbit anti-MreB antibodies for MreB detection. 5 µl stationary phase cultures of MC1000 Δ*mreBCD*, pTK554, pKG339 (before depletion) and MC1000 Δ*mreBCD* were loaded as +ve and –ve controls respectively. For

depletion, cells were diluted 1/100 in 25 ml LB with 10 μg/ml tetracycline. 0.2 mM IPTG was used to induce depletion at time 0. Samples between 5 and 10 ml were taken every 30 min through the time course, pelleted and re-suspended in water. Protein concentration of each sample was assayed and matched amounts loaded onto each lane, with the maximum possible volume used. **(C)** *E. coli* MC1000 cell width measurements with MreB and MreB^{D285A} overexpression from pAKF128 (P_{BAD}::*mreBCD*) and pAKF129 (P_{BAD}::*mreB*^{D285A}*CD*) compared to an empty vector control (pBAD24). Cells were grown in M9 medium with (+) or without (-) 0.000,05% arabinose inducer at 30^{o}C for 5 h prior to imaging. Error bars show +/- standard deviation. In all cases there was no significant difference between populations (t-test, p>0.05). **(D)** Representative bright field micrographs showing *E. coli* MC1000 cells containing: pBAD24, pAKF128 or pAKF129 MreB/MreB^{D285A} over expression constructs. Scale bar = 5 μm. Six hundred and seventy cells were sampled for each condition and represent the same cells whose length measurements are shown in Figure 3B(ii), n=3.

Figure S5. MreB^{D285A}-compensating FtsZ variant bacterial two hybrid binding profiles and phenotypes.

(A) Representative images of BTH101 double transformation plates. Transformants were grown on NA plates containing selective antibiotics and X-gal (40 μg/ml). In each case the pKNT25-ftsZ mutant plasmids (pAKF135-140, horizontal) were used as bait against the pUT18C-mreB, pUT18C-mreB^{D285A} and pUT18C-ftsZ vectors used to express T18- constructs (vertical). Values shown in brackets are representative of the bacterial two hybrid signal strength summarised in Figure 4A; ++ = strong binding signal, + = weaker binding signal, - = no detectable signal. Each image is representative of at least two independent repeats. **(B)** FtsZ complementation screen for FtsZ variants identified in this study. *E. coli* VIP205 stain

(P_{tac}::*ftsZ*) carrying plasmids pAKF134-pAKF140 (P_{tet}::*ftsZ* +point mutants) were gown to stationary phase in LB with antibiotics at 30^{o}C + 30 µM IPTG. Cultures were serially diluted 1/10 in LB and 5 µl of each dilution was replica spotted onto NA plates containing antibiotics and either: 30 µM IPTG (left) 'No FtsZ Depletion' or 20 ng/ml chlortetracycline (right) 'FtsZ Replacement'. Plates shown are from the same experiment and are representative of four independent repeats which gave identical results. Values shown in brackets are representative of each FtsZ variant ability to complement the Δ*ftsZ* phenotype where: ++ = full- (comparable to *ftsZ*^{wt} complementation control), + = partial (100 drop in CFU compared to *ftsZ*^{WT} control)- and - = no complementation (same CFU as –ve empty vector contol); these scores are shown in Figure 4A. **(C)** FtsZ mutants can complement MreB^{D285A} overexpression. *E. coli* VIP205 (P_{tac}::*ftsZ*) cells were grown without IPTG inducer giving FtsZ depletion. This was complemented by expression of FtsZ from pAKF135 (P_{tet}::*ftsZ*) or pAKF137 (P_{tet}::*ftsZ*^{P203Q}) induced using 20 ng/ml chlorotetracycline. Strains contained either pAKF128 (P_{BAD}::*mreBCD*) or pAKF129 (P_{BAD}::*mreB*^{D285A}*CD*) induced with 0.005% arabinose for controlled MreB overexpression. Cells were grown in M9 media for 8 h, serially diluted 1/10 and 5 µl spotted onto NA plates with antibiotics and 30 µM IPTG. These plates gave viable counts of the liquid cultures independent of the MreB or FtsZ mutant phenotypes. **(i)** The FtsZ^{P203Q} mutant can complement MreB^{D285A} overexpression. Expression of MreB^{D285A} reduces CFU as cells start to elongate (Compare viability when MreB^{WT} or MreB^{D285A} is overexpressed and the FtsZ^{wt} allele is used for VIP205 complementation, red arrows). Using FtsZ^{P203Q} for VIP205 complementation in cells over expressing MreB^{WT} reduces cell viability. Whereas FtsZ^{P203Q} complementation of VIP205 in cells overexpressing MreB^{D285A} gives higher CFU counts (Compare viability when MreB^{WT} or MreB^{D285A} is overexpressed and FtsZ^{P203Q} allele is used for VIP205 complementation, green arrows). **(ii)** All MreB^{D285A} binding

FtsZ mutants can complement MreB^{D285A} overexpression. Note all FtsZ mutants give higher CFU counts that either FtsZ^{WT} or the empty vector control. Plate images are representative of three independent repeats (n=3). **(D)** Representative micrographs of *E. coli* VIP205 (P_{tac}::*ftsZ*) cells grown without inducer. Cells were complemented by expressing either *ftsZ* or *ftsZ*^{P203Q} from pAKF135 or pAKF137 respectively, induced using 20 ng/ml chlorotetracycline. Cells were grown in M9 media for 5 h at 30^{o}C, transferred to a 1% agarose pad and imaged immediately. Scale bar = 5 µm.

Figure S6. Nucleoid separation and PBP1A-mCherry signal distribution are unaffected by MreB^{D285A} induced cell elongation. FtsI-inhibited Z rings can still incorporate HADA cell wall label. *E. coli* MC1000 cells expressing MreB^{D285A} form pAKF129 (P_{BAD}::*mreB*^{D285A}*CD*), MreB^{WT} from pAKF128 (P_{BAD}::*mreBCD*) or empty vector control (pBAD24). **(A,B)** Representative images of *E. coli* MC1000, pAKF133 (P_{BAD}::*ftsZ-mCherry*) cells. Merged bright field and FtsZ-mCherry fluorescence images are shown with corresponding Hoechst DNA fluorescence image below (cyan). FtsZ rings form between segregated bacterial nucleoids in MreB^{D285A} elongated cells **(B)** and controls **(A)** -indicated using white dashed arrows. **(C)** Fixed HADA fluorescent D-amino acid labelled cells. MC1000 pAKF133 cells were grown for 2 h in M9 media at 30^{o}C, treated with 1 µg/ml aztreonam and allowed to grow for an additional 1.5 h. Aztreonam inhibits PBP3 and blocks cell division, causing cells to elongate. Cells were incubated with 1 mM HADA for 30 s, fixed using 70% ethanol and washed in PBS before microscopy. Note: HADA label is incorporated at aztreonam-inhibited Z rings, suggesting that pre-septal synthesis has occurred at these sites. **(D)** MC100 empty vector (pBAD24) and MreB^{WT} (pAKF128) controls also expressing PBP1A-mCherry from pAKF143

(P_{lac}::*mrcA-mCherry*); signal distributions are recorded for both non-dividing (i) and dividing cells (ii) the site of septation is indicated using red arrows. **(E)** MC1000 pAKF129 $MreB^{D285A}$ elongated cells expressing PBP1A-mCherry from pAKF143. PBP1A forms punctate membrane-associated foci in non-dividing cells and is not localised to cell division sites. Note in all cases the distribution patters of all tagged proteins were identical in MreB 'over-expression' and empty vector control cells. All cells were grown in M9 media at 30^{o}C with 0.000,05% arabinose inducer before microscopy. Images are representative of at least two independent repeats. Scale bar = 2 µm.

Figure S7. Representative images of mCherry-tagged cell division and elongation factors in MC1000 empty-vector and MreB 'over-expression' controls. *E. coli* MC1000 cells expressing MreB from the pAKF128 vector (P_{BAD}::*mreBCD*) or empty vector control (pBAD24). In addition cells are expressing fluorescently tagged cell morphogenesis proteins from a second plasmid to study the localisation patterns of these proteins *in vivo* **(A)** Merged bright field and fluorescent images showing mid-cell Z ring localisation in cells expressing FtsZ-mCherry from the pAKF133 plasmid (P_{BAD}::*ftsZ-mCherry*). **(B,C)**
PBP1B and PBP2 signal distributions in both non-dividing (i) and dividing cells (ii), fluorescent tags were expressed from plasmids, pAKF145 (P_{lac}::*mrcB-mCherry*) or pAKF146 (P_{lac}::*mrdA-mCherry*) respectively. PBP1B and PBP2 form punctate membrane-associated foci in non-dividing cells and are also localised to cell division sites, in contrast to PBP1A (see Figure S6D,E). The location of septa in dividing cells is highlighted – red arrows. **(D,E)** Membrane-associated PBP3 and FtsN are localised to mature septum in dividing cells – red arrows. PBP3-mCherry was expressed from the pAKF147 plasmid (P_{lac}::*ftsI-mCherry*) and FtsN-mCherry from the pAKF150 (P_{lac}::*mCherry-ftsN*). Note in all cases the distribution patters of

all tagged proteins were identical in MreB 'over-expression' and empty vector control cells. All cells were grown in M9 media for 5 h at 30^{o}C with 0.000,05% arabinose inducer before microscopy. Images are representative of at least two independent repeats. Scale bar = 2 μm.

Figure S8. Representative images of mCherry-tagged cell division and elongation factors in MC1000 cells treated with a PBP3-inhibitor. *E. coli* MC1000 cells expressing fluorescently tagged cell morphogenesis proteins from plasmids: pAKF143 (P_{lac}::*mrcA-mCherry*) **(A)**, pAKF145 (P_{lac}::*mrcB-mCherry*) **(B)**, pAKF146 (P_{lac}::*mrdA-mCherry*) **(C)**, pAKF147 (P_{lac}::*ftsI-mCherry*) **(D)** or pAKF150 (P_{lac}::*mCherry-ftsN*) **(E)**. Stationary phase cultures were diluted 1/100 into M9 media and incubated at 30^{o}C for 2 h. 1 μg/ml aztreonam (A,C-E) or cephalexin (B) was used to inhibit PBP3(FtsI), arresting cell division and leading to cell elongation. Typically cells were incubated at 30^{o}C for 1.5 h before microscopy to allow elongation. This treatment resulted in multiple stalled 'mature' divisomes in elongated cells unable to divide. In this assay, inhibited divisomes contained: PBP1B, PBP2, PBP3 (inhibited although still localised) and FtsN but lacked PBP1A (see red arrows). Note: these localisation results are consistent with *wt* localisation patters observed in Figures S6D and S7. Note: PBP1B and PBP2 form bands or ring-like structures in inhibited cells which contrasts to the localisation pattern observed in MreB^{D285A} elongated cells shown in Figure 5C,D. Images are representative of at least two independent repeats. Scale bar = 2 μm.

Figure S9. Time-lapse series showing MreB recruitment to the Z-ring in *E. coli*. Time-lapse series of bright field and fluorescent micrographs following MG1655 cells expressing the mYpet-MreB and FtsZ-mCherry recombinant proteins from plasmids pAKF106 (P_{BAD}::*mYpet-*

mreBCD) and pQW59 (P_{lac}::*ftsZ-mCherry*). Arrows indicate the location and co-localisation of major mYpet-MreB foci and FtsZ-mCherry rings. For each example, a single cell division event is shown. The mYpet-MreB signal migrates to the new division plane either one frame behind **(A)** or simultaneously with **(B)** Z-ring establishment. Images were acquired every 2.5 min and are shown at 1 frame per second. The first and last frames were duplicated for clarity.

Figure S10. Time-lapse series showing atypical MreB-Z-ring recruitment events in *E. coli*. Time-lapse series of bright field and fluorescent micrographs following MG1655 cells expressing the mYpet-MreB and FtsZ-mCherry recombinant proteins from plasmids pAKF106 (P_{BAD}::*mYpet-mreBCD*) and pQW59 (P_{lac}::*ftsZ-mCherry*). Arrows indicate the location and co-localisation of major mYpet-MreB foci and FtsZ-mCherry rings. Rare localisation patterns and mYpet-MreB behaviours are shown. **(A)**, a cell with no initial MreB-FtsZ signal overlap switched to MreB-FtsZ co-localisation after the Z-ring migrates to two new sites. **(B)**, an abortive Z-ring (lower ring) migrates to a new site within the same cell without any clear cell invagination, taking the major mYpet-MreB signal with it. **(C)**, a rare elongated cell showing Z ring migration intermediates that co-localise with mYpet-MreB signals (lower ring, migrating downwards). The second Z-ring both maintains the mYpet-MreB co-localisation (upper ring, migrating downwards) and loses the co-localisation (upper ring, migrating upwards). Images were acquired every 2.5 min and are shown at 1 frame per second. The first and last frames were duplicated for clarity.

Figure S11. Time-lapse series following mCherry-tagged PBPs in *mreB*^{D285A}*CD* expressing cells. Examples of both elongated (left) and dividing cells (right) are shown. **(A)** PBP1A-

mCherry forms foci which migrate along the cell periphery in both elongated and dividing cells. PBP1A is not recruited to the cell division site. **(B, C)** PBP1B-mCherry and PBP2-mCherry form membrane-associated foci which migrate along the cell periphery. In dividing cells bright foci are also observed forming rings or bands at the septum – white arrows. These structures are absent from $MreB^{D285A}$ elongated cells. **(D)** PBP3-mCherry is membrane bound and forms bright foci associated with the division septum – white arrows. PBP3-mCherry is recruited to inhibited-septa in $MreB^{D285A}$ elongated cells – see grey arrows for selected examples. These structures can persist for long periods of time but eventually disperse without initiating cell division. All cells were grown in M9 media for 5 h at 30^{o}C with 0.000,05% arabinose inducer before microscopy. In the case of pAKF146 M9 glucose media and 0.1% arabinose was used to control expression. Time-lapses are representative of at least four independent repeats. Images were acquired every 2.5 min and are shown at 1.2 frames per second. The first and last frame has been duplicated for clarity. Scale bar = 2 μm.

Table SI – Strains and Plasmids used in this study

Strains

Name	Genotype	Resistance Marker	Source or Reference
BL21(DE3)	*E. coli* B strain: F$^-$, *dcm, ompT, hsdS*(r_B^- m_B^-), *gal*, λDE3(*lac*I *lac*UV5-T7 gene 1, *ind*1, *sam*7, *nin*5)	-	Invitrogen
BTH101	F,$^-$ *cya*-99, *ara*D139, *gal*E15, *gal*K16, *rps*L1, *hsd*R2, *mcr*A1, *mcr*B1	-	Karimova and Ladant
DH5α	*fhuA2, Δ(argF-lacZ)U169, phoA glnV44, Φ80, Δ(lacZ)M15, gyrA96, recA1, relA1, endA1, thi-1, hsdR17*	-	Derivative of DH5 (Hanahan, 1983)
FB76	TB28: *mreB'-mCherry-'mreB yhdE<>cat*	Chloramphenicol	(Bendezú *et al*, 2009)
MC1000	*F-, Δ(araA-leu)7697*, *[araD139]$_{B/r}$*, *Δ(codB-lacI)3*, *galK16*, *galE15*(GalS), *λ*$^-$, *e14-*, *relA1*, *rpsL150*(strR), *spoT1*, *mcrB1*	-	(Casadaban & Cohen, 1980)
MC1000 *Δmre*	MC1000: *Δmre*	Chloramphenicol	(Kruse *et al*, 2005)
MC1000 *ΔmreB*	MC1000: *ΔmreB*	Chloramphenicol	(Kruse *et al*, 2005)
MC1061	*araD39, Δ(araA-leu)7697, ΔlacX74, galU*$^-$, *galK*$^-$, *hsr*$^-$, *hsm+, strA*	-	(Casadaban & Cohen, 1980)
MG1655	K12 type-strain: F$^-$, *λ*$^-$, *rph-1*	-	Laboratory Collection (Jensen, 1993)
PS106	W3110: *ftsZ84 leu::*Tn*10* (Ts)	-	(Pichoff & Lutkenhaus, 2005)
PS236	W3110: *ftsA12 leu::*Tn*10* (Ts)	-	(Pichoff & Lutkenhaus, 2002)
TB28	MG1655: *lacIZYA<>frt*	-	(Bernhardt & De Boer, 2003)
VIP205	MC1061: P_{tac}::*ftsZ*, lacI^q	Kanamycin	(Garrido *et al*, 1993)

Plasmids

Name	Relevant Genotypes /Notes	Replicon	Resistance Marker	Source or Reference
pAKF100	P_{BAD}::*mypet* / cloning vector	pACYC	Chloramphenicol	This study
pAKF106	P_{BAD}::*mypet-mreBCD*	pACYC	Chloramphenicol	This study
pAKF126	P_{lac}::*his$_8$-mreB*(D285A), *lacI*^{q}	pUC	Ampicillin	This study
pAKF128	P_{BAD}::*mreBCD*	pMB1 (*rop*$^-$)	Ampicillin	This study
pAKF129	P_{BAD}::*mreB*(D285A)*CD*	pMB1 (*rop*$^-$)	Ampicillin	This study
pAKF130	P_{BAD}::*mypet-mreB*(D285A)*CD*	pACYC	Chloramphenicol	This study
pAKF131	P_{BAD}::*mypet-mreBCD*	pMB1	Ampicillin	This study
pAKF132	P_{BAD}::*mypet-mreB*(D285A)*CD*	pMB1	Ampicillin	This study
pAKF133	P_{BAD}::*ftsZ-mCherry*	pACYC	Chloramphenicol	This study
pAKF134	P_{tet} cloning vector	pACYC	Chloramphenicol	This study
pAKF135	P_{tet}::*ftsZ*	pACYC	Chloramphenicol	This study
pAKF136	P_{tet}::*ftsZ*(P203R)	pACYC	Chloramphenicol	This study
pAKF137	P_{tet}::*ftsZ*(P203Q)	pACYC	Chloramphenicol	This study
pAKF138	P_{tet}::*ftsZ*(T296A)	pACYC	Chloramphenicol	This study
pAKF139	P_{tet}::*ftsZ*(D301N)	pACYC	Chloramphenicol	This study
pAKF140	P_{tet}::*ftsZ*(M302L)	pACYC	Chloramphenicol	This study
pAKF142	P_{lac}::-*mCherry*, *lacI*^{q}, cloning vector (C-terminal fusions)	pACYC	Chloramphenicol	This study

Name	Relevant Genotypes /Notes	Replicon	Resistance Marker	Source or Reference
pAKF143	P_{lac}::*mrcA-mCherry*, *lacI*^{q}	pACYC	Chloramphenicol	This study
pAKF145	P_{lac}::*mrcB-mCherry*, *lacI*^{q}	pACYC	Chloramphenicol	This study
pAKF146	P_{lac}::*mrdA-mCherry*, *lacI*^{q}	pACYC	Chloramphenicol	This study
pAKF147	P_{lac}::*ftsI-mCherry*, *lacI*^{q}	pACYC	Chloramphenicol	This study
pAKF149	P_{lac}::*mCherry-*, *lacI*^{q} cloning vector (N-terminal fusions)	pACYC	Chloramphenicol	This study
pAKF150	P_{lac}::*mCherry-ftsN*, *lacI*^{q}	pACYC	Chloramphenicol	This study
pBAD24	P_{BAD} /cloning vector	pMB1 (*rop*$^-$)	Ampicillin	(Guzman *et al*, 1995) (Cronan, 2006)
pBAD322	P_{BAD} /cloning vector	pMB1	Ampicillin	(Cronan, 2006)
pDSW230	P_{lac}:: *ftsZ-gfp*, *lacI*^{q}	pMB1	Ampicillin	(Weiss *et al*, 1999)
pKG339	P_{lac}::*copA*	pSC101	Tetracycline	(Jensen *et al*, 1995)
pKNT25	P_{lac}::-*T25*	pACYC	Kanamycin	(Karimova *et al*, 2005)
pKNT25-ftsZ	P_{lac}::*ftsZ-T25*	pACYC	Kanamycin	(Karimova *et al*, 2005)
pKNT25-ftsZ(P203R)	P_{lac}::*ftsZ*(P203R)-*T25*	pACYC	Kanamycin	This study
pKNT25-ftsZ(P203Q)	P_{lac}::*ftsZ*(P203Q)-*T25*	pACYC	Kanamycin	This study
pKNT25-ftsZ(T296A)	P_{lac}::*ftsZ*(T296A)-*T25*	pACYC	Kanamycin	This study
pKNT25-ftsZ(D301N)	P_{lac}::*ftsZ*(D301N)-*T25*	pACYC	Kanamycin	This study
pKNT25-ftsZ(M302L)	P_{lac}::*ftsZ*(M302L)-*T25*	pACYC	Kanamycin	This study
pKNT25-*rodZ*	P_{lac}::*rodZ-T25*	pACYC	Kanamycin	This study
pKT25	P_{lac}::*T25-*	pACYC	Kanamycin	(Karimova *et al*, 2001)
pKT25-ftsA	P_{lac}::*T25-ftsA*	pACYC	Kanamycin	(Karimova *et al*, 2005)
pKT25-ftsB	P_{lac}::*T25-ftsB*	pACYC	Kanamycin	(Karimova *et al*, 2005)
pKT25-ftsI	P_{lac}::*T25-ftsI*	pACYC	Kanamycin	(Karimova *et al*, 2005)
pKT25-ftsL	P_{lac}::*T25-ftsL*	pACYC	Kanamycin	(Karimova *et al*, 2005)
pKT25-ftsN	P_{lac}::*T25-ftsN*	pACYC	Kanamycin	(Karimova *et al*, 2005)
pKT25-ftsQ	P_{lac}::*T25-ftsQ*	pACYC	Kanamycin	(Karimova *et al*, 2005)
pKT25-ftsW	P_{lac}::*T25-ftsW*	pACYC	Kanamycin	(Karimova *et al*, 2005)
pKT25-ftsX	P_{lac}::*T25-ftsX*	pACYC	Kanamycin	(Karimova *et al*, 2005)
pKT25-ftsZ$_{1-383}$	P_{lac}::*T25-ftsZ*	pACYC	Kanamycin	This study
pKT25-mreB	P_{lac}::*T25-mreB*	pACYC	Kanamycin	This study
pKT25-mreB(ΔN)	P_{lac}::*T25-mreB*$_{9-347}$	pACYC	Kanamycin	This study
pKT25-zapA	P_{lac}::*T25-zapA*	pACYC	Kanamycin	(Galli & Gerdes, 2010)
pKT25-zip	P_{lac}::*T25-leucine zipper region from yeast GCN4.*	pACYC	Kanamycin	(Karimova *et al*, 2001)
pMFV56	P_{lac}::*ftsZ, lacI*^{q}	pMB1, f1	Kanamycin	(Rivas *et al*, 2000)
pT25-mreB(D285A)	P_{lac}::*T25-mreB*(D285A)	pACYC	Chloramphenicol	This study
pTK500	P_{lac}::*his*$_8$*-mreB, lacI*^{q}	pUC	Ampicillin	(Kruse *et al*, 2003)
pTK549	P_{mre}::*mreBCD*	mini-R1	Kanamycin	(Kruse *et al*, 2005)
pTK554	P_{lac}::*T25-mreB*	pACYC	Chloramphenicol	(Kruse *et al*, 2005)
pTK559	P_{lac}::*T18-mreB*	pUC	Ampicillin	(Kruse *et al*, 2005)
pTK560	P_{lac}::*T25-mreC*	pACYC	Chloramphenicol	(Kruse *et al*, 2005)
pUT18	P_{lac}::-*T18*	pUC	Ampicillin	(Karimova *et al*, 2001)
pUT18-ftsZ	P_{lac}::*ftsZ-T18*	pUC	Ampicillin	This study
pUT18C	P_{lac}::*T18-*	pUC	Ampicillin	(Karimova *et al*, 2001)

Name	Relevant Genotypes /Notes	Replicon	Resistance Marker	Source or Reference
pUT18C-ftsA	P_{lac}::*T18-ftsA*	pUC	Ampicillin	(Karimova *et al*, 2005)
pUT18C-ftsB	P_{lac}::*T18-ftsB*	pUC	Ampicillin	(Karimova *et al*, 2005)
pUT18C-ftsI	P_{lac}::*T18-ftsI*	pUC	Ampicillin	(Karimova *et al*, 2005)
pUT18C-ftsL	P_{lac}::*T18-ftsL*	pUC	Ampicillin	(Karimova *et al*, 2005)
pUT18C-ftsN	P_{lac}::*T18-ftsN*	pUC	Ampicillin	(Karimova *et al*, 2005)
pUT18C-ftsQ	P_{lac}::*T18-ftsQ*	pUC	Ampicillin	(Karimova *et al*, 2005)
pUT18C-ftsW	P_{lac}::*T18-ftsW*	pUC	Ampicillin	(Karimova *et al*, 2005)
pUT18C-ftsX	P_{lac}::*T18-ftsX*	pUC	Ampicillin	(Karimova *et al*, 2005)
pUT18C-ftsZ	P_{lac}::*T18-ftsZ*	pUC	Ampicillin	(Ebersbach *et al*, 2006)
pUT18C-mreB	P_{lac}::*T18-mreB*	pUC	Ampicillin	This study
pUT18C-mreB(ΔN)	P_{lac}::*T18-mreB*$_{9-347}$	pUC	Ampicillin	This study
pUT18C-mreB(D285A)	P_{lac}::*T18-mreB*(D285A)	pUC	Ampicillin	This study
pUT18C-zapA	P_{lac}::*T18-zapA*	pUC	Ampicillin	(Galli & Gerdes, 2010)
pUT18C-zip	P_{lac}::*T18-leucine zipper region from yeast GCN4.*	pUC	Ampicillin	(Karimova *et al*, 2001)
pQW59	P_{lac}::*ftsZ*::*mCherry*, *lacI*^{q}	pUC	Ampicillin	This study

Supplementary References

Arai R, Ueda H, Kitayama A, Kamiya N & Nagamune T (2001) Design of the linkers which effectively separate domains of a bifunctional fusion protein. *Protein engineering* **14:** 529–32

Bendezú FO, Hale CA, Bernhardt TG & De Boer PAJ (2009) RodZ (YfgA) is required for proper assembly of the MreB actin cytoskeleton and cell shape in E. coli. *The EMBO Journal* **28:** 193–204

Bernhardt TG & De Boer PAJ (2003) The Escherichia coli amidase AmiC is a periplasmic septal ring component exported via the twin-arginine transport pathway. *Molecular Microbiology* **48:** 1171–1182

Biles BD & Connolly BA (2004) Low-fidelity Pyrococcus furiosus DNA polymerase mutants useful in error-prone PCR. *Nucleic acids research* **32:** e176

Casadaban MJ & Cohen SN (1980) Analysis of gene control signals by DNA fusion and cloning in Escherichia coli. *Journal of molecular biology* **138:** 179–207

Cronan JE (2006) A family of arabinose-inducible Escherichia coli expression vectors having pBR322 copy control. *Plasmid* **55:** 152–7

Ebersbach G, Ringgaard S, Møller-Jensen J, Wang Q, Sherratt DJ & Gerdes K (2006) Regular cellular distribution of plasmids by oscillating and filament-forming ParA ATPase of plasmid pB171. *Molecular microbiology* **61:** 1428–42

Van den Ent F, Amos LA & Löwe J (2001) Prokaryotic origin of the actin cytoskeleton. *Nature* **413:** 39–44

Galli E & Gerdes K (2010) Spatial resolution of two bacterial cell division proteins: ZapA recruits ZapB to the inner face of the Z-ring. *Molecular microbiology* **76:** 1514–26

Galli E & Gerdes K (2012) FtsZ-ZapA-ZapB interactome of Escherichia coli. *Journal of bacteriology* **194:** 292–302

Garrido T, Scnchez M, Palacios P, Aldea M & Vicente M (1993) Transcription of ftsZ oscillates during the cell cycle of Esherichia coli. *The EMBO Journal* **12:** 3957–65

Guzman LM, Belin D, Carson MJ, Beckwith J, Guzman L, Belin D & Carson MJ (1995) Tight regulation , modulation , and high-level expression by vectors containing the arabinose PBAD promoter . **177:**

Hanahan D (1983) Studies on transformation of Escherichia coli with plasmids. *Journal of molecular biology* **4:** 557–80

Ishikawa S, Kawai Y, Hiramatsu K, Kuwano M & Ogasawara N (2006) A new FtsZ-interacting protein, YlmF, complements the activity of FtsA during progression of cell division in Bacillus subtilis. *Molecular microbiology* **60:** 1364–80

Jensen KF (1993) The Escherichia coli K-12 “wild types” W3110 and MG1655 have an rph frameshift mutation that leads to pyrimidine starvation due to low pyrE expression levels. *Journal of bacteriology* **175:** 3401–7

Jensen RB, Grohmann E, Schwab H, Diaz-Orejas R & Gerdes K (1995) Comparison of ccd of F, parDE of RP4, and parD of R1 using a novel conditional replication control system of plasmid R1. *Molecular microbiology* **17:** 211–220

Karimova G, Dautin N & Ladant D (2005) Interaction Network among Escherichia coli Membrane Proteins Involved in Cell Division as Revealed by Bacterial Two-Hybrid Analysis. *Journal of Bacteriology* **187:** 2233–43

Karimova G, Ullmann A & Ladant D (2001) Protein-Protein Interaction Between Bacillus stearothermophilus Tyrosyl-tRNA Synthetase Subdomains Revealed by a Bacterial Two-Hybrid System. **3:** 73–82

Kruse T, Bork-Jensen J & Gerdes K (2005) The morphogenetic MreBCD proteins of Escherichia coli form an essential membrane-bound complex. *Molecular microbiology* **55:** 78–89

Kruse T, Møller-Jensen J, Løbner-Olesen A & Gerdes K (2003) Dysfunctional MreB inhibits chromosome segregation in Escherichia coli. *The EMBO journal* **22:** 5283–92

Kuru E, Hughes HV, Brown PJ, Hall E, Tekkam S, Cava F, De Pedro MA, Brun Y V & Vannieuwenhze MS (2012) In Situ Probing of Newly Synthesized Peptidoglycan in Live Bacteria with Fluorescent D-Amino Acids. *Angewandte Chemie* **51:** 12519–23

Miller JH (1972) Experiments in molecular genetics, Cold Spring Harbor Press

Nguyen AW & Daugherty PS (2005) Evolutionary optimization of fluorescent proteins for intracellular FRET. *Nature biotechnology* **23:** 355–60

Pichoff S & Lutkenhaus J (2002) Unique and overlapping roles for ZipA and FtsA in septal ring assembly in Escherichia coli. *The EMBO journal* **21:** 685–93

Pichoff S & Lutkenhaus J (2005) Tethering the Z ring to the membrane through a conserved membrane targeting sequence in FtsA. *Molecular microbiology* **55:** 1722–34

Rivas G, Lopez A, Mingorance J, Ferrandiz MJ, Zorrilla S, Minton AP, Vicente M & Andreu JM (2000) Magnesium-induced Linear Self-association of the FtsZ Bacterial Cell Division Protein Monomer. *The Journal of biological chemistry* **275:** 11740–11749

Weiss DS, Chen JC, Ghigo J, Beckwith J & Boyd D (1999) Localization of FtsI (PBP3) to the Septal Ring Requires Its Membrane Anchor, the Z Ring, FtsA, FtsQ, and FtsL. *Journal of bacteriology* **181(2):** 508–520

Zacharias DA, Violin JD, Newton AC & Tsien RY (2002) Partitioning of lipid-modified monomeric GFPs into membrane microdomains of live cells. *Science* **296:** 913–6

Figure S1

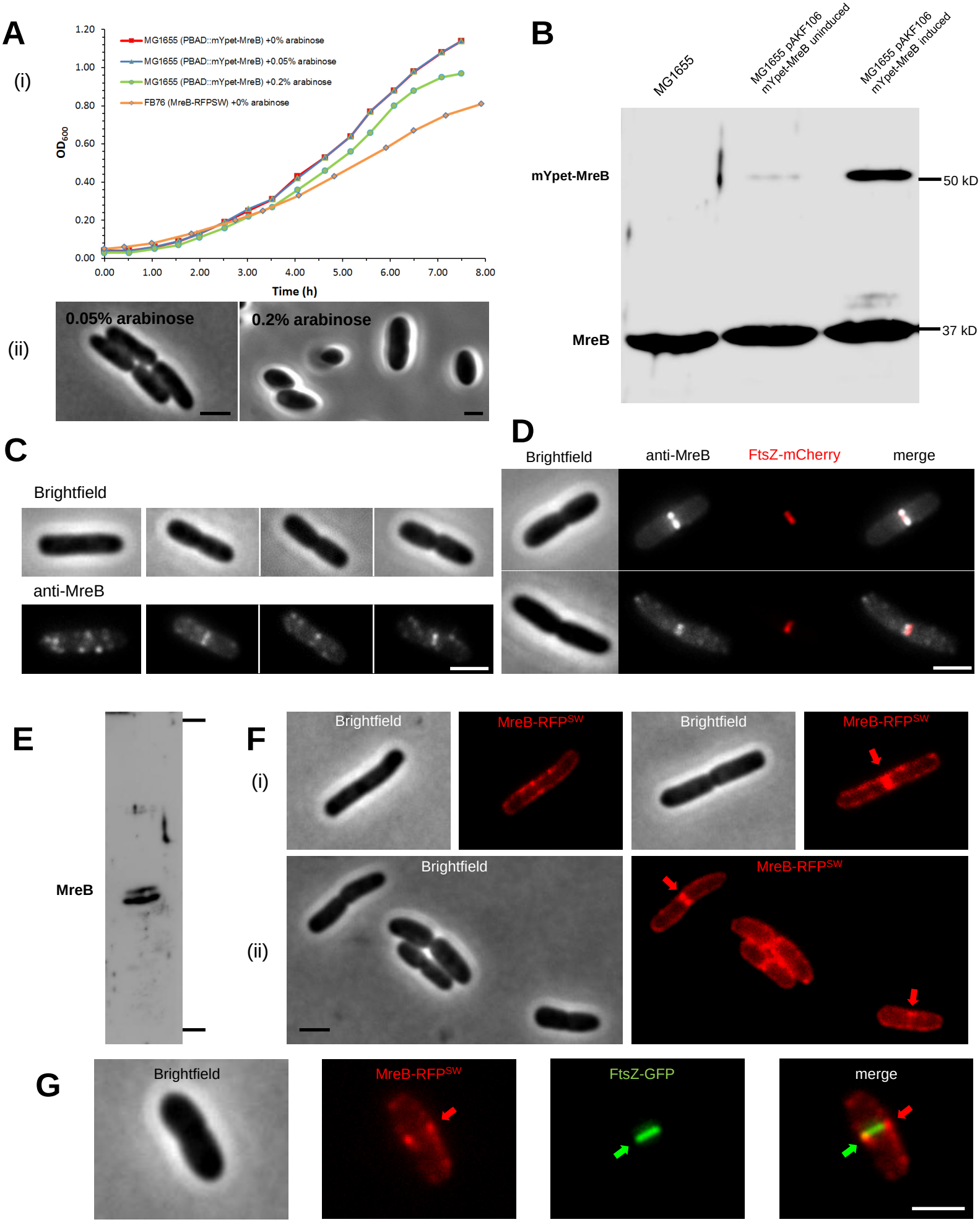
A
(i)
MG1655 (PBAD::mYpet-MreB) +0% arabinose
MG1655 (PBAD::mYpet-MreB) +0.05% arabinose
MG1655 (PBAD::mYpet-MreB) +0.2% arabinose
FB76 (MreB-RFPSW) +0% arabinose
OD600
Time (h)
(ii)
0.05% arabinose
0.2% arabinose
B
MG1655
MG1655 pAKF106 mYpet-MreB uninduced
MG1655 pAKF106 mYpet-MreB induced
mYpet-MreB
MreB
50 kD
37 kD
C
Brightfield
anti-MreB
D
Brightfield
anti-MreB
FtsZ-mCherry
merge
E
MreB
F
(i)
Brightfield
MreB-RFPSW
(ii)
G
Brightfield
MreB-RFPSW
FtsZ-GFP
merge

Figure S2

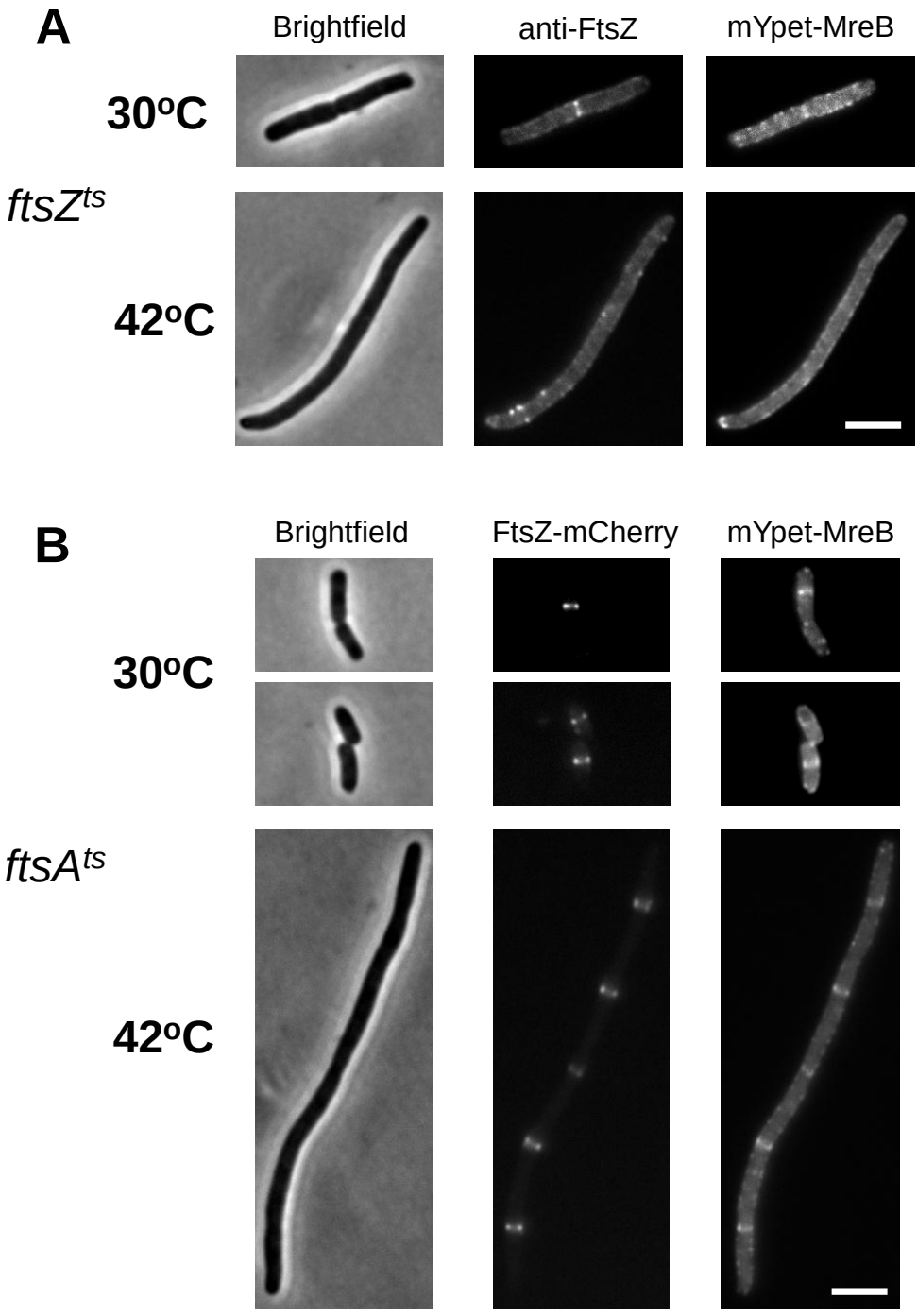
A
Brightfield
anti-FtsZ
mYpet-MreB
30ºC
ftsZts
42ºC
B
Brightfield
FtsZ-mCherry
mYpet-MreB
30ºC
ftsAts
42ºC

Figure S3

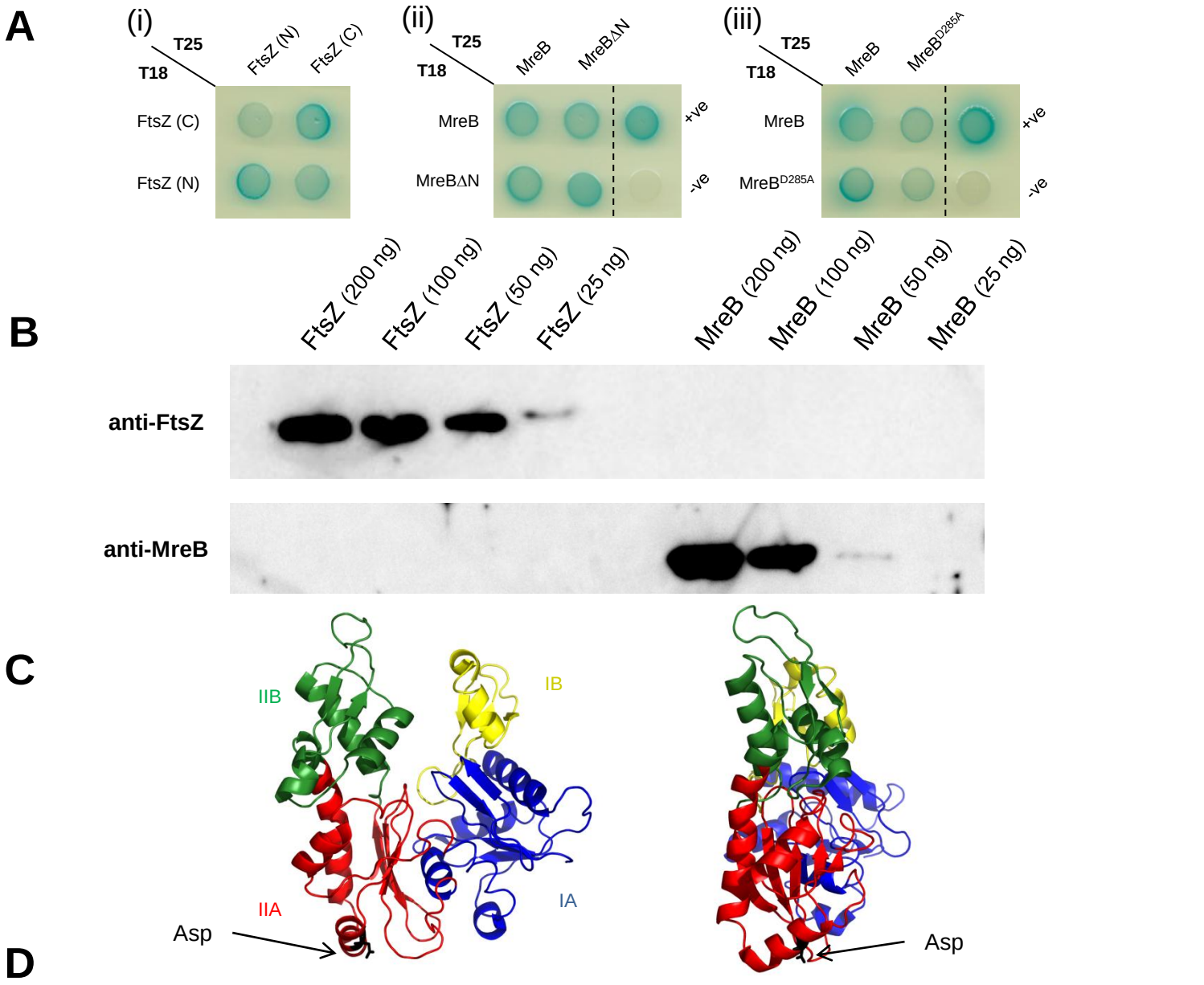
A
(i)
T25
T18
FtsZ (N)
FtsZ (C)
FtsZ (C)
FtsZ (N)
(ii)
T25
T18
MreB
MreBΔN
MreB
MreBΔN
+ve
-ve
(iii)
T25
T18
MreB
MreB^D285A
MreB
MreB^D285A
+ve
-ve
B
FtsZ (200 ng)
FtsZ (100 ng)
FtsZ (50 ng)
FtsZ (25 ng)
MreB (200 ng)
MreB (100 ng)
MreB (50 ng)
MreB (25 ng)
anti-FtsZ
anti-MreB
C
IIB
IB
IIA
IA
Asp
Asp
D
Dilution
1 2 3 4 5 6 7
Arabinose concentration
0%
0.000,05%
0.000,5%
empty vector
MreB
MreB^D285A
Dilution
1 2 3 4 5 6 7
0.005%
0.05%
0.2%
empty vector
MreB
MreB^D285A

Figure S4

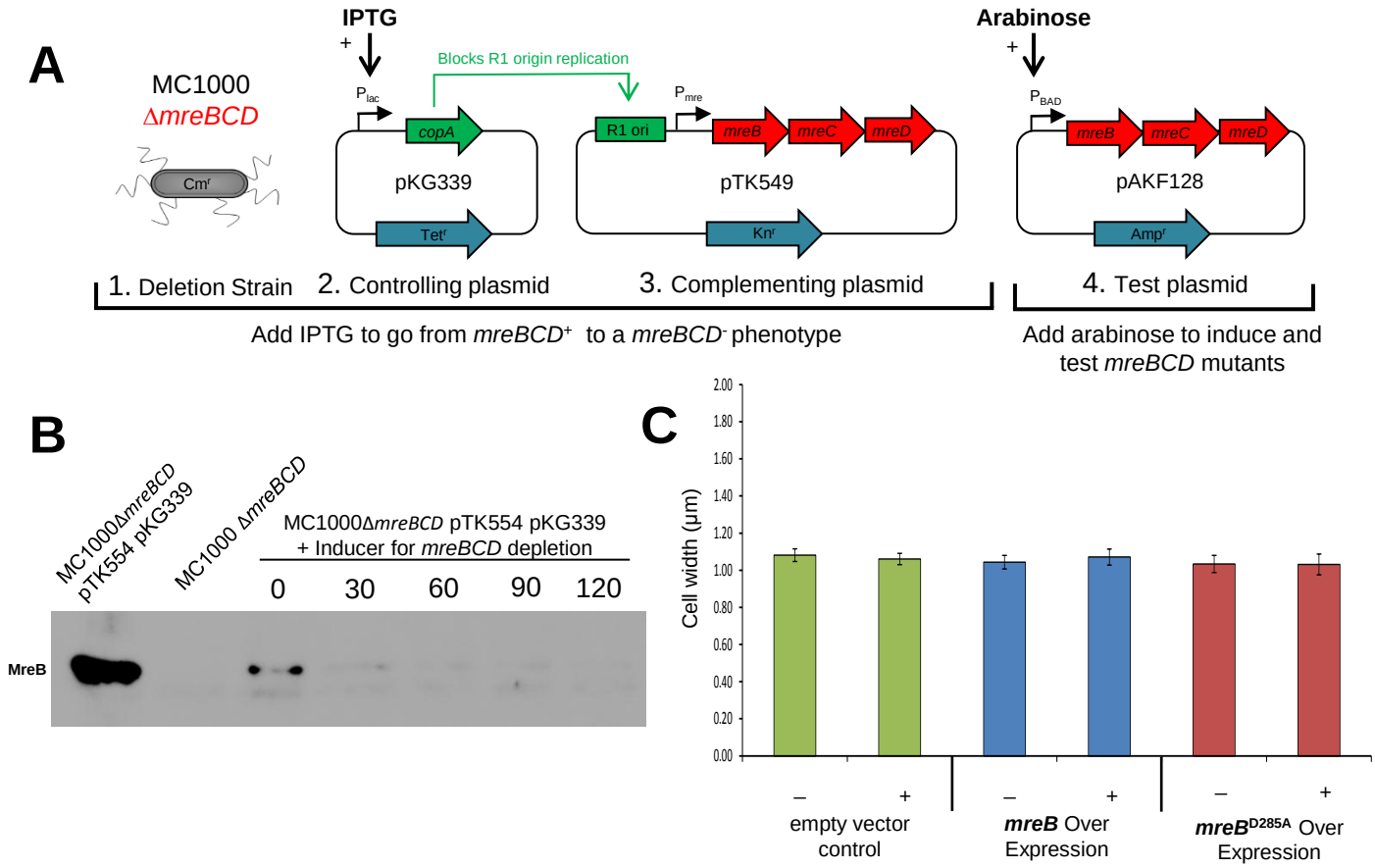
A
MC1000
ΔmreBCD
Cmr
IPTG
+
Blocks R1 origin replication
Plac
copA
pKG339
Tetr
R1 ori
Pmre
mreB
mreC
mreD
pTK549
Knr
Arabinose
+
PBAD
mreB
mreC
mreD
pAKF128
Ampr
1. Deletion Strain
2. Controlling plasmid
3. Complementing plasmid
4. Test plasmid
Add IPTG to go from mreBCD+ to a mreBCD- phenotype
Add arabinose to induce and test mreBCD mutants

B
MC1000ΔmreBCD pTK554 pKG339
MC1000 ΔmreBCD
MC1000ΔmreBCD pTK554 pKG339
+ Inducer for mreBCD depletion
0
30
60
90
120
MreB

C
Cell width (µm)
2.00
1.80
1.60
1.40
1.20
1.00
0.80
0.60
0.40
0.20
0.00
–
+
empty vector control
mreB Over Expression
mreBD285A Over Expression

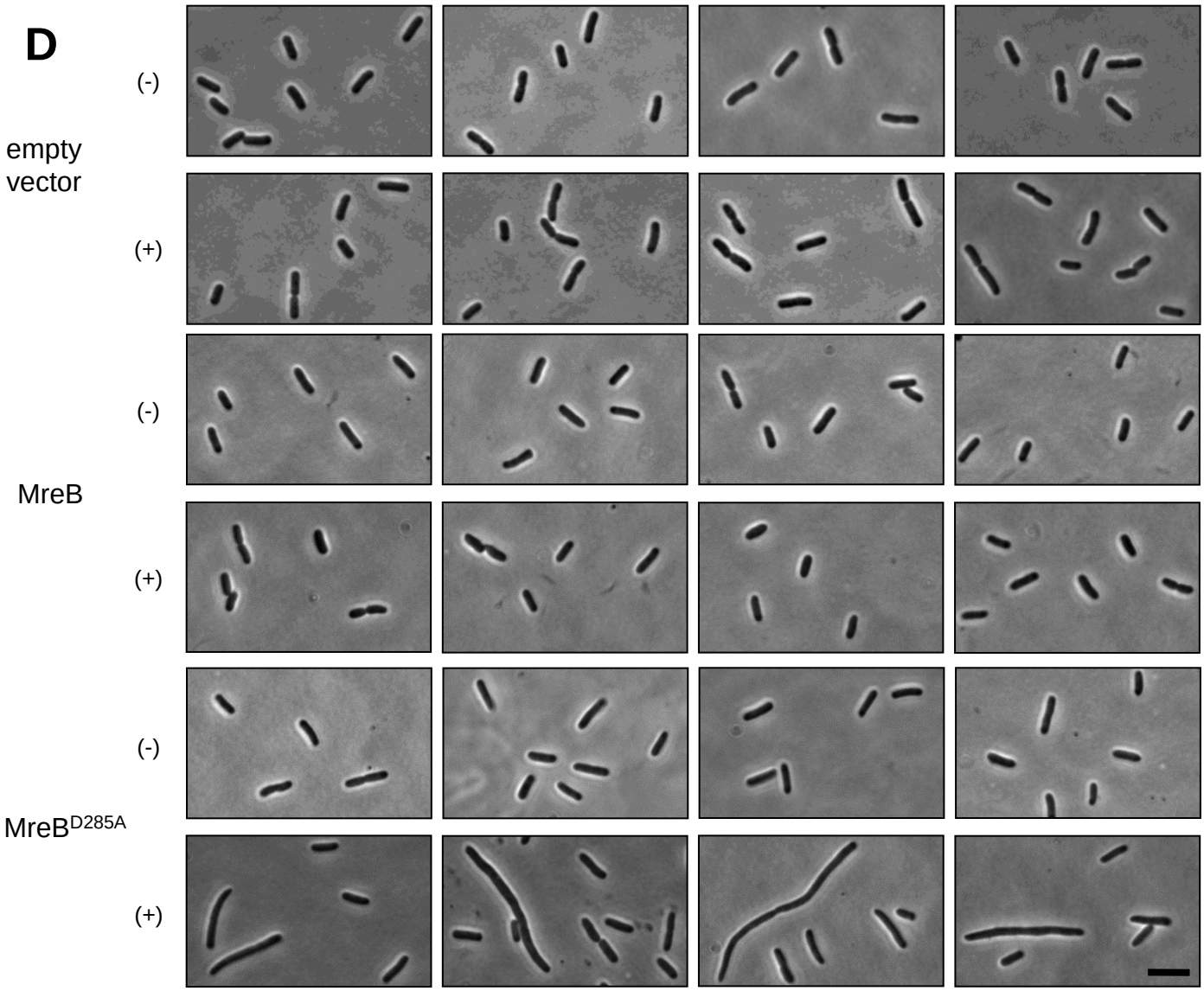
D
(-)
empty vector
(+)
(-)
MreB
(+)
(-)
MreBD285A
(+)

Figure S5

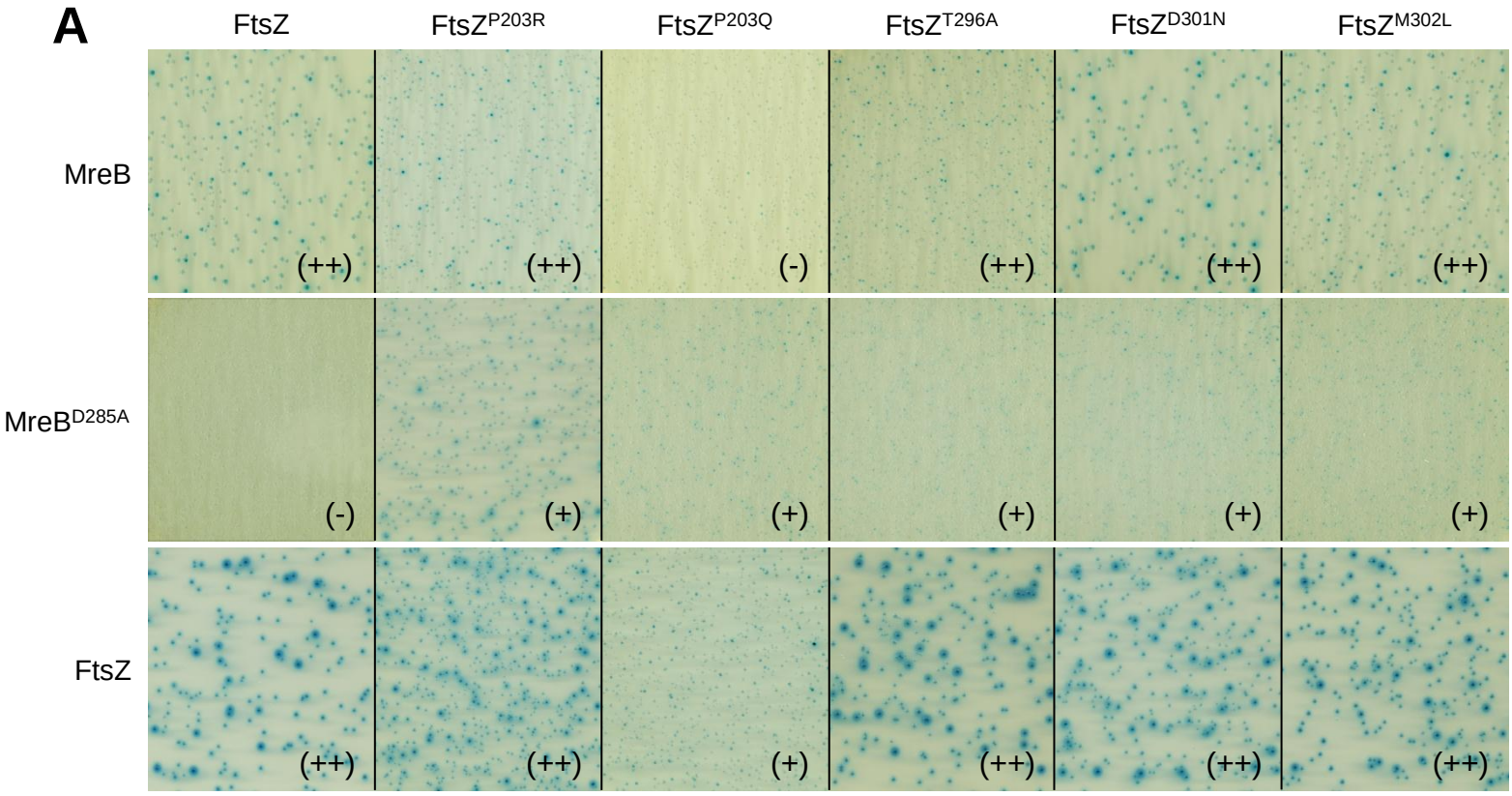
A
FtsZ
FtsZ^P203R
FtsZ^P203Q
FtsZ^T296A
FtsZ^D301N
FtsZ^M302L
MreB
MreB^D285A
FtsZ
(++) (++) (-) (++) (++) (++)
(-) (+) (+) (+) (+) (+)
(++) (++) (+) (++) (++) (++)

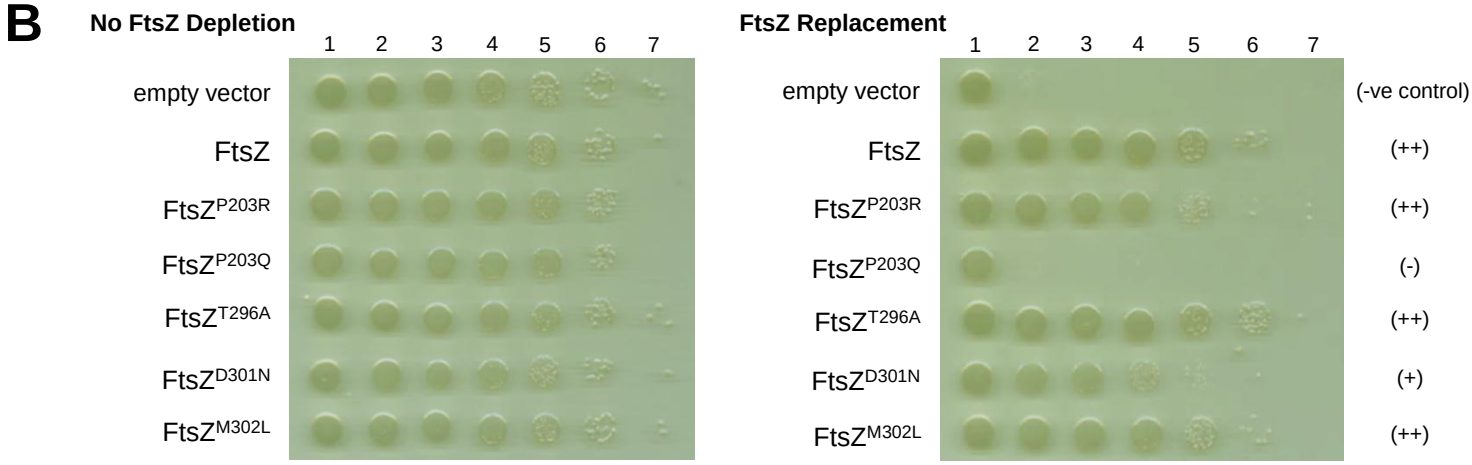
B
No FtsZ Depletion
FtsZ Replacement
1 2 3 4 5 6 7
empty vector
FtsZ
FtsZ^P203R
FtsZ^P203Q
FtsZ^T296A
FtsZ^D301N
FtsZ^M302L
(-ve control)
(++)
(++)
(-)
(++)
(+)
(++)

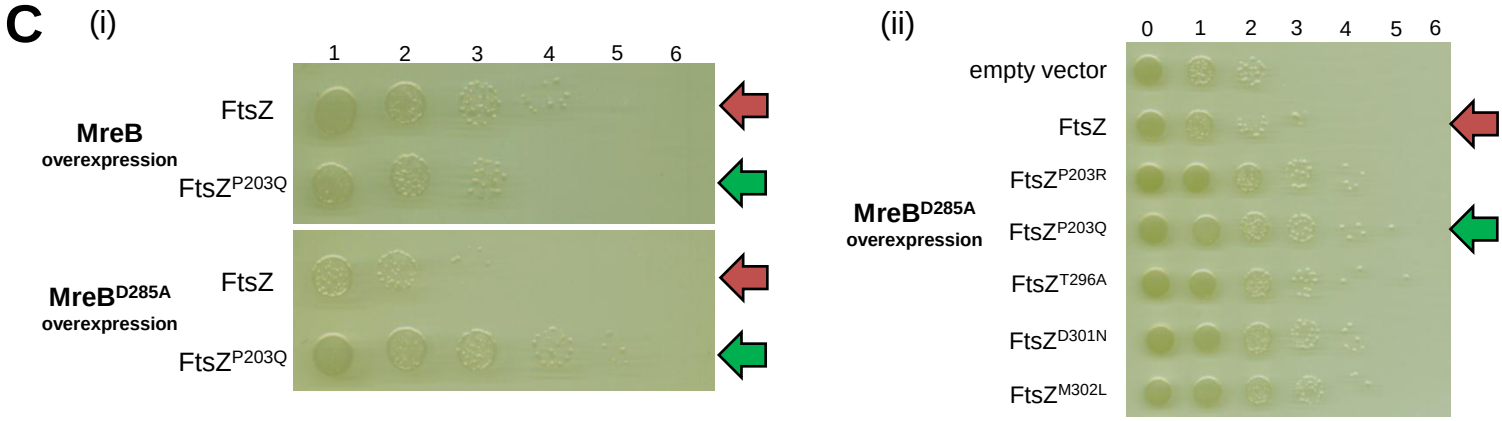
C
(i)
1 2 3 4 5 6
MreB overexpression
MreB^D285A overexpression
FtsZ
FtsZ^P203Q
(ii)
0 1 2 3 4 5 6
empty vector
FtsZ
FtsZ^P203R
FtsZ^P203Q
FtsZ^T296A
FtsZ^D301N
FtsZ^M302L
MreB^D285A overexpression

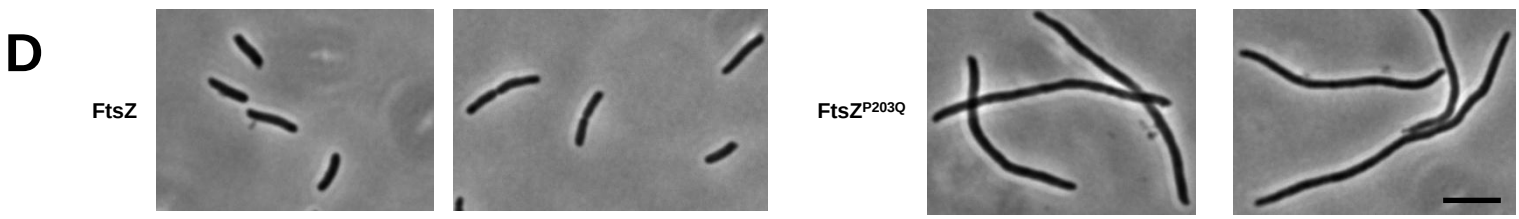
D
FtsZ
FtsZ^P203Q

Figure S6

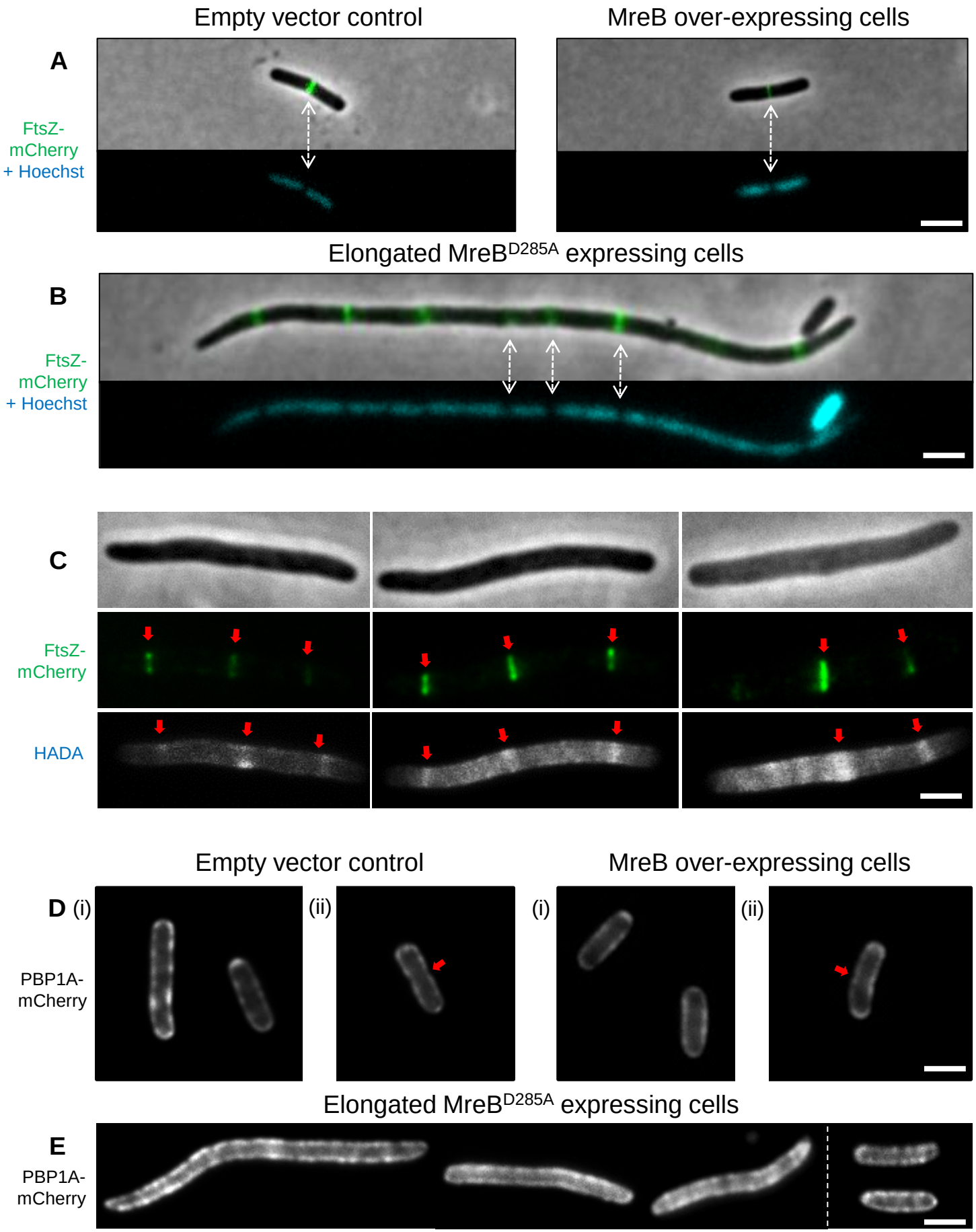
Empty vector control
MreB over-expressing cells
A
FtsZ-mCherry + Hoechst
Elongated MreB^{D285A} expressing cells
B
FtsZ-mCherry + Hoechst
C
FtsZ-mCherry
HADA
Empty vector control
MreB over-expressing cells
D (i)
(ii)
(i)
(ii)
PBP1A-mCherry
Elongated MreB^{D285A} expressing cells
E
PBP1A-mCherry

Figure S7

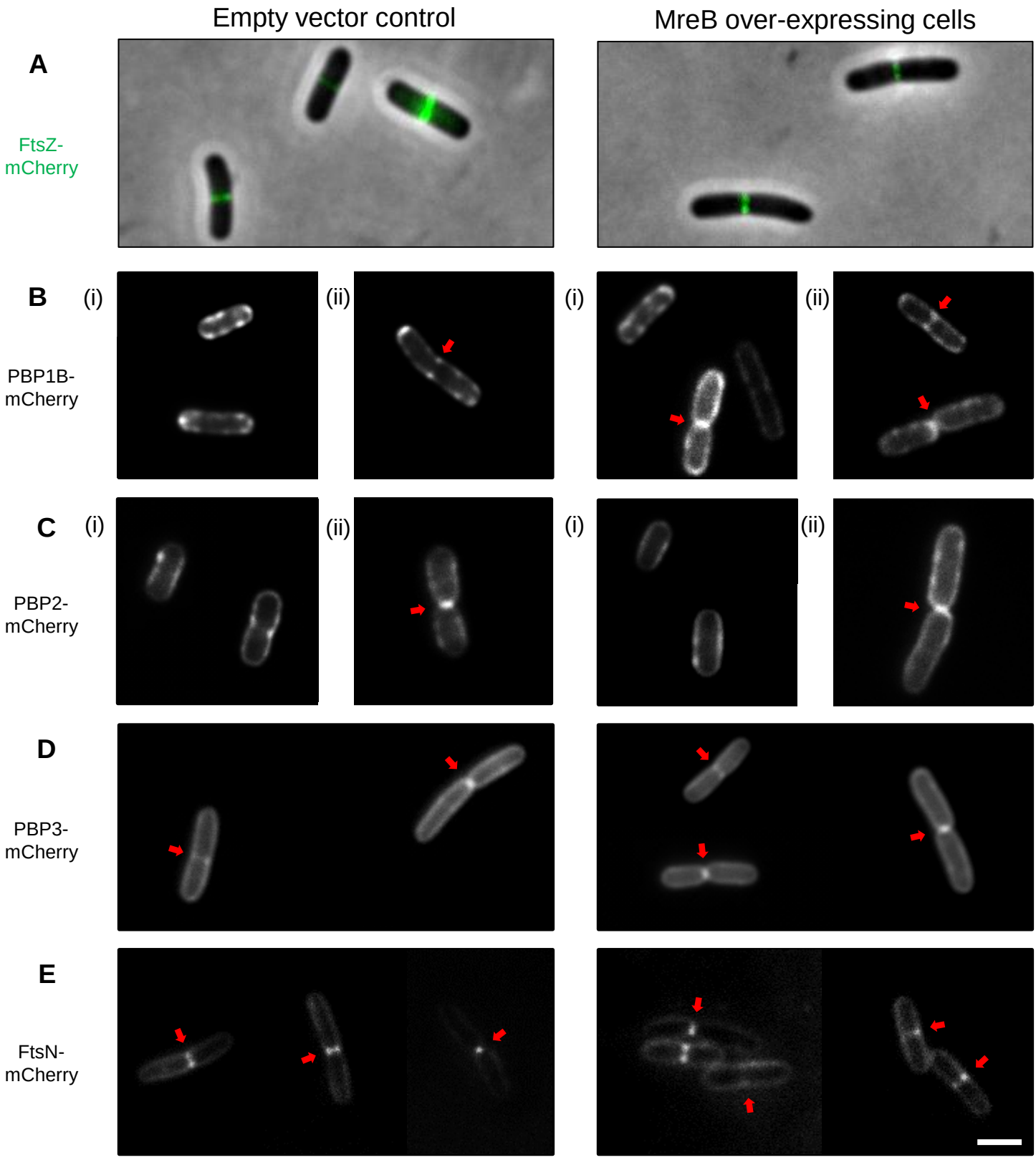
Empty vector control
MreB over-expressing cells
A
FtsZ-mCherry
B
(i)
(ii)
PBP1B-mCherry
C
PBP2-mCherry
D
PBP3-mCherry
E
FtsN-mCherry

Figure S8

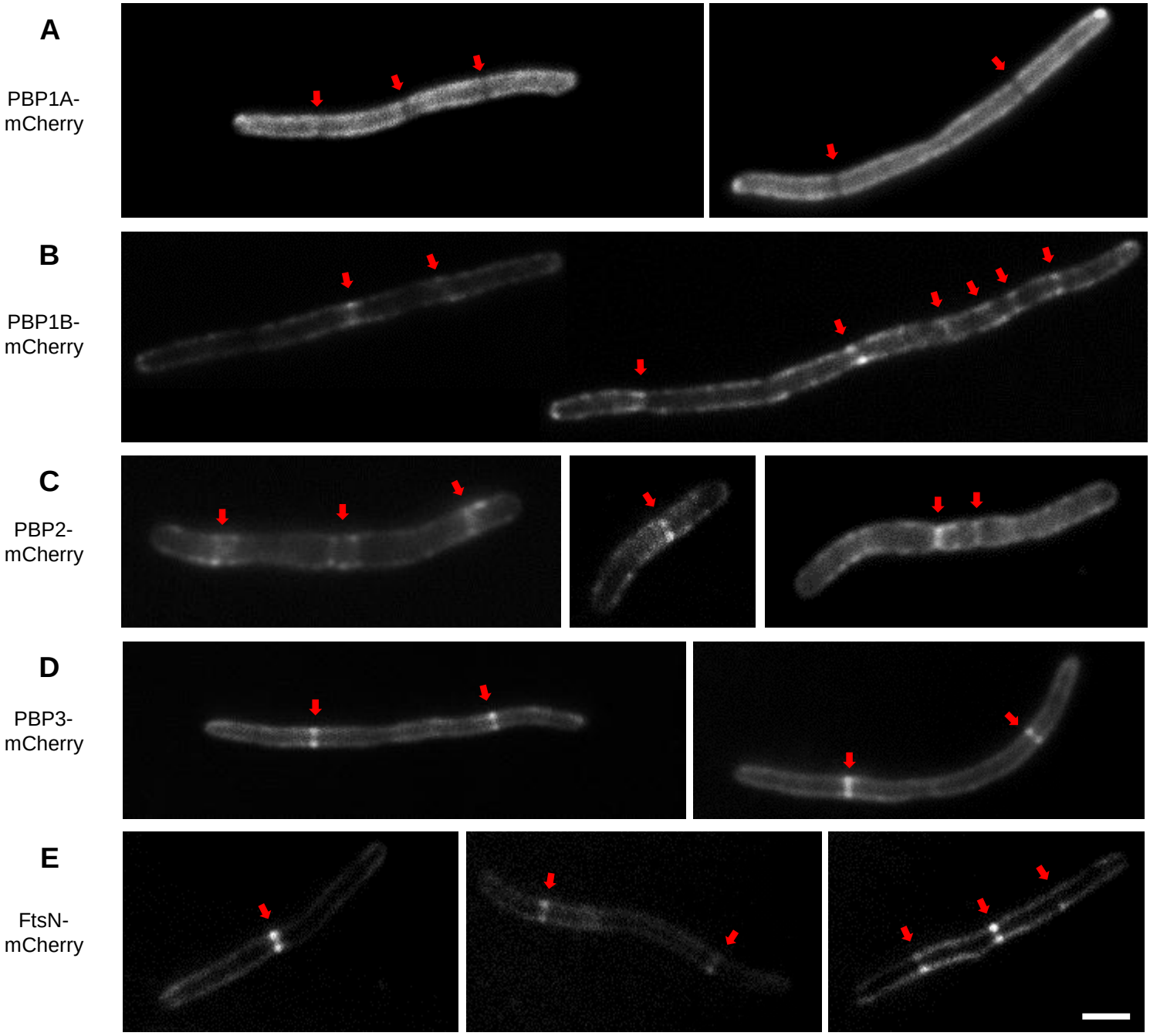
A
PBP1A-mCherry
B
PBP1B-mCherry
C
PBP2-mCherry
D
PBP3-mCherry
E
FtsN-mCherry